Molecular Basis of Peripheral vs Central Benzodiazepine Receptor Selectivity in a New Class of Peripheral Benzodiazepine Receptor Ligands Related to Alpidem

Maurizio Anzini,[‡] Andrea Cappelli,*[,‡] Salvatore Vomero,[‡] Gianluca Giorgi,[†] Thierry Langer,[§] Giancarlo Bruni,[⊥] Maria R. Romeo,[⊥] and Anthony S. Basile[∥]

Dipartimento Farmaco Chimico Tecnologico, Università di Siena, Via Banchi di Sotto 55, 53100 Siena, Italy, Centro Interdipartimentale di Analisi e Determinazioni Strutturali, Università di Siena, via P.A. Mattioli 10, 53100 Siena, Italy, Institute of Pharmaceutical Chemistry, University of Innsbruck, Innrain 52A, A-6020 Innsbruck, Austria, Istituto di Farmacologia, Università di Siena, Le Scotte 6, 53100 Siena, Italy, and Laboratory of Neuroscience, NIDDKD, National Institutes of Health, Bethesda, Maryland 20892

Received April 30, 1996[⊗]

Alpidem (**1**), the anxiolytic imidazopyridine, has nanomolar binding affinity for both the central benzodiazepine receptor (CBR) and the peripheral benzodiazepine receptor (PBR). A novel class of PBR ligands related to alpidem has been designed by comparing the interaction models of alpidem with PBR and CBR. Several compounds in this class have shown high selectivity for PBR vs CBR, and the selectivity has been discussed in terms of interaction models. The binding behavior of the three selected compounds was extensively studied by competition and saturation assays, and the results suggest that they are capable of recognizing two sites labeled by [^{3}H]PK11195. The molecular structure of one of the most active compounds (**4e**) has been determined by X-ray diffraction and compared with that of alpidem. Molecular modeling studies suggest that the bioactive conformation of **4e** is likely to be very similar to the conformation found in the crystal.

Introduction

Since their discovery, benzodiazepines have attracted the attention of researchers owing to their potential and actual clinical uses and because of their low toxicity. The efforts made in this field have led to the development of many clinical important anxiolytics, anticonvulsants, hypnotics, and muscle relaxants and to the discovery of the benzodiazepine receptor itself.

Soon after its description, it was found that a number of structurally different classes of substances could bind to the benzodiazepine receptor.[1] Moreover, benzodiazepine receptors have been found both in the central nervous system (CNS) and in peripheral tissues[2] and have subsequently been divided into two classes: the central and peripheral benzodiazepine receptors. The central benzodiazepine receptor (CBR) is localized only on the cell membrane of neurons, where it is part of the γ-aminobutyric acid ($GABA_A$) receptor complex, and is involved in the regulation of GABA-gated chloride ion currents. In contrast, the peripheral benzodiazepine receptor (PBR) is located in both CNS and peripheral tissues. Although PBR are found primarily on the mitochondrial outer membrane, a nonmitochondrial localization in some cells has also been suggested.[3]

While the physiological function of the PBR is not fully understood (for recent reviews, see refs 3 and 4), it is clearly not involved in the regulation of chloride currents. The PBR do appear to be involved in steroidogenesis, the regulation of which is a potential clinical application of PBR selective compounds.[5]

Alpidem (**1**) binds with nanomolar affinity both PBR (K_i = 0.5−7 nM) and CBR (K_i = 1−28 nM)[6] and stimulates pregnenolone formation from mitochondria of C6-2B glioma cells.[6b] The anxiolytic and anticonvulsant properties of **1** appear to be elicited both with a direct mechanism through the interaction with CBR and with an indirect mechanism by the interaction with PBR and neurosteroid production.[5,6b,c] Compound **2**, a close derivative of alpidem, also stimulates pregnenolone formation, but it appears to be more selective for the PBR than alpidem, as it shows nanomolar affinity for the PBR (K_i = 3.9 nM) and no significant affinity for the CBR (IC_{50} > 1000 nM).[5] Related compounds, such as zopiclone (**3**)[7] and **3a**,[8] show significant affinity for the CBR (IC_{50} = 29 and 380 nM, respectively) with little or no affinity for the PBR. We have been interested for

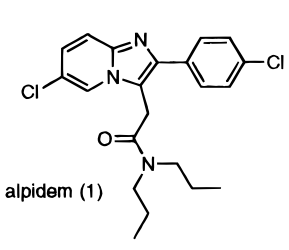

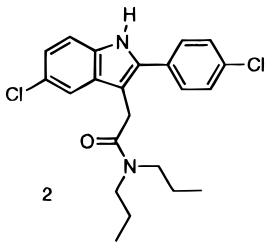

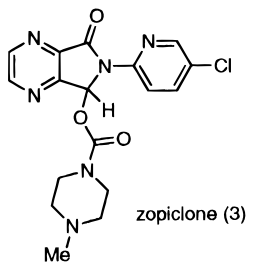

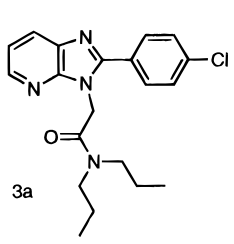

[‡] Dipartimento Farmaco Chimico Tecnologico.
[†] Centro Interdipartimentale di Analisi e Determinazioni Strutturali.
[§] University of Innsbruck.
[⊥] Istituto di Farmacologia.
[∥] NIDDKD, National Institutes of Health.
[⊗] Abstract published in *Advance ACS Abstracts,* August 15, 1996.

S0022-2623(96)00325-1 CCC: $12.00

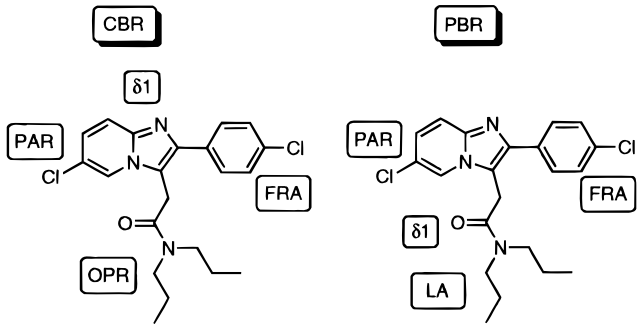

Figure 1. Comparison between the schematic representation of the interaction models of alpidem with CBR and PBR.

several years in chemically modifying nonselective ligands to produce more selective compounds and have successfully applied our efforts to different classes of CNS agents.[9] In this paper we describe the results obtained when alpidem was chosen as the lead compound. The design, synthesis, biological evaluation, and molecular modeling studies of a new class of potent and selective PBR ligands are reported. These compounds should be of particular interest in the light of the fact that PBR would appear to offer an indirect pharmacological approach to modulation of $GABA_A$ receptor complex.[6d]

Drug Design

The rational design of selective ligands from a nonselective mother compound implies the knowledge of key pharmacophoric elements in the interaction with the different receptors. These elements can be deduced from the available structure−activity relationship (SAR) studies. In the present study, a survey of the literature has revealed the existence of at least three models for the interactions of benzodiazepines with the CBR (Fryer,[1] Wermuth,[7] and Borea[10]) and two interaction models for PBR.[6,11] The three CBR interaction models analyzed are very similar and readily integrated into one comprehensive model. Figure 1 shows an integrated model for the interaction of alpidem with the CBR, which takes into account the agonist properties of alpidem. Furthermore, this model was obtained following similar topological and electronic guiding criteria previously used (see refs 1, 7, and 10) in the model development. The different zones were termed using the nomenclature proposed by Wermuth: FRA, freely rotating aromatic ring region, corresponding to A in Fryer's model and to AG1 in Borea's model; δ1, electron-rich zone, corresponding to π1 in Fryer's model and to B1 in Borea's model; OPR, out-plane region, corresponding to π3 in Fryer's model and to AG2 in Borea's model; and PAR, planar aromatic region.

Bourguignon has conceived an interaction model for the PBR very similar to that for CBR[6] with some important differences in the spatial location of the main pharmacophoric points. Comparison of the interaction models for the PBR and CBR (Figure 1) predicts that prevention of the imidazole nitrogen from behaving as the H-bond acceptor in alpidem should decrease the compound's affinity for CBR. This concept served as the basis for the design of the PBR selective compound **2**,[5] where the geometry of alpidem was conserved, but the H-bond acceptor imidazole nitrogen was converted into a H-bond donor indole nitrogen.

The lack of CBR affinity of compound **2** confirms the importance of the imidazole nitrogen atom of alpidem for the interaction with CBR and suggests at the same time a limited role of the acetamide side chains in CBR interaction, while the carbonyl dipole and amide lipophilic side chains are important for interaction with the PBR.[5] Thus, the acetamide moiety became the target for further structural modifications aimed at enhancing PBR selectivity.

Compounds **4**−**7** and **13** were designed as structural hybrids of alpidem and zopiclone, maintaining the minimum requisites for the interaction with both the PBR and CBR while varying the geometry and lipophilicity of the side chains. In addition, the comparative ability of the PBR and CBR to accommodate large heteroaromatic portions was explored by the bioisosteric replacement of 5-chlorine substituent of alpidem with a condensed benzo ring.

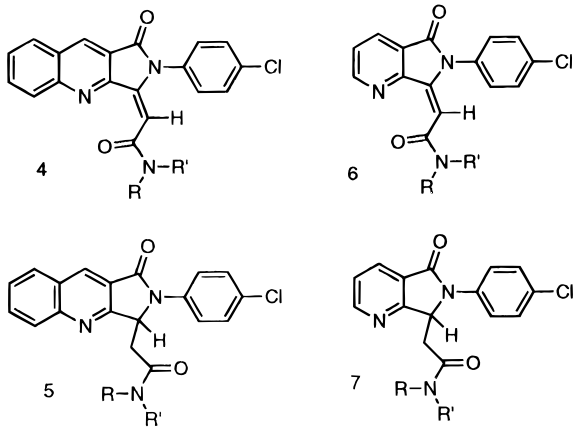

Chemistry

The synthesis of the title compounds was performed from pyrrolo[3,4-*b*]quinoline **11** or pyrrolo[3,4-*b*]pyridine **18** through the attack of their active methylene groups with different electrophilic alkylating agents as the key steps.

In Scheme 1 the synthesis of ylideneacetic derivatives **4a**−**f** starting from aniline is reported. Aniline (**8**) was condensed with ethyl 4-chloroacetoacetate and ethyl anilinobutenoate intermediate **9** was subjected to Vilsmeier formilation conditions[12] to give quinoline **10**. Compound **10** was then reacted with *p*-chloroaniline in ethanol to reflux to give key intermediate **11** in 92% yield, which was used without further purification.

Condensation between **11** and glyoxylic acid monohydrate in glacial acetic acid and acetic anhydride (1:1) afforded unsaturated acid **12** in 59% yields. The *E*-geometry of the exocyclic double bond of **12** was assigned in the first instance on the basis of low-field resonance of the carboxylic proton (16.13 ppm) observed in ^{1}H-NMR spectrum of **12** in deuterated chloroform. It was assumed that an intramolecular hydrogen bond between the carboxylic hydrogen and quinoline nitrogen atom stabilizes the *E*-geometry of acid **12**.

The unsaturated acid **12** was converted into the corresponding amides **4a**−**f** via mixed anhydrides. When the conversion of unsaturated acid **12** into the corresponding *N*,*N*-dipropyl amide was carried out via acid chloride, a partial inversion of configuration at the exocyclic double bond was observed. The major product (yield 55%) of this reaction showed *Z*-geometry (**13**),

Scheme 1[a]

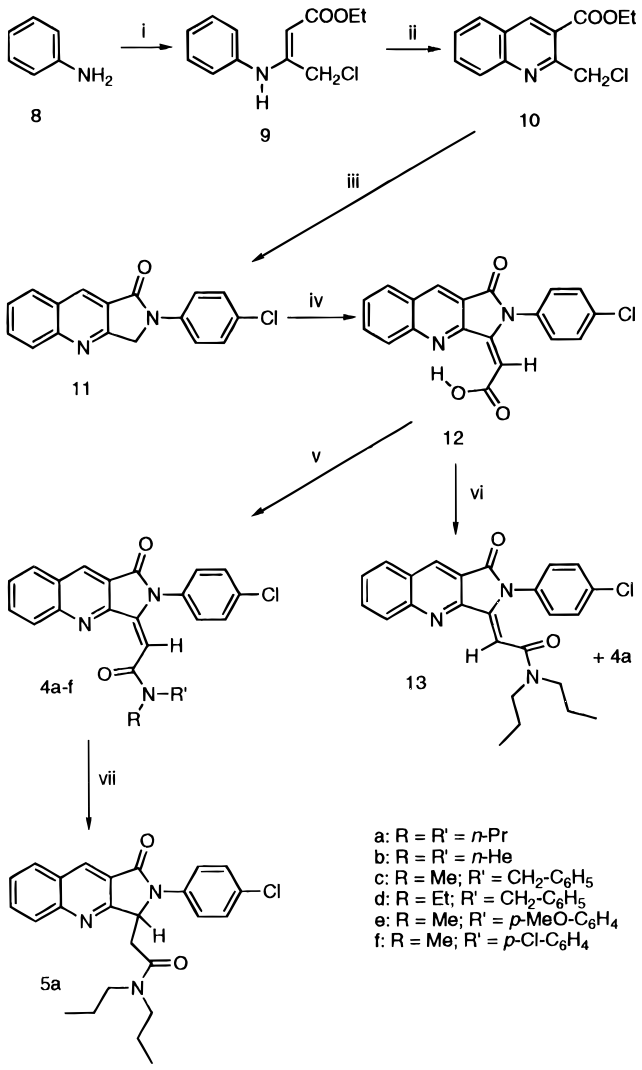

[a] Reagents: (i) $ClCH_2COCH_2COOEt$, AcOH, C_6H_6; (ii) DMF, $POCl_3$, $CHCl_3$; (iii) p-$ClC_6H_4NH_2$, EtOH; (iv) $CHOCOOH \cdot H_2O$, Ac_2O, AcOH; (v) i-BuOCOCl, Et_3N, RNHR′ (method A or B); (vi) $SOCl_2$, n-Pr_2NH, MeC_6H_5; (vii) H_2, Pd/C, EtAc.

while the *E*-isomer (**4a**) was isolated only in 14% yield. *E*−*Z*-Geometry of the amides **4** and **13** was assigned on the basis of their ^{1}H-NMR spectra in comparison with that of starting acid **12** for which *E*-geometry was assumed. Finally, single-crystal X-ray diffraction studies performed on compound **4e** confirmed unequivocally the *E*-geometry for this compound and the basic assumption mentioned above.

Catalytic reduction of compound **4a** gave only trace amount of expected **5a**; thus, a different approach to the synthesis of saturated amides **5a**,**b** was investigated (Scheme 2). Sodium hydride has been reported to be effective in deprotonating a pyrrolo[3,4-*b*]quinoline system very similar to **11** to give a resonance-delocalized anion which could be alkylated with butyl iodide.[13]

Unfortunately, the attempts at the direct alkylation of the anion generated from **11** using NaH in DMF with ethyl bromoacetate were unsuccessful; however, the anion could be acylated using dimethyl carbonate to give ester **14** in 92% yield. Compound **14** was deprotonated in anhydrous DMF by DBU to give a dark blue-colored anion which was alkylated with ethyl bromoacetate to diester **15**, characterized by its ^{1}H-NMR spectrum and used without further purification. Hydrolysis of the

Scheme 2[a]

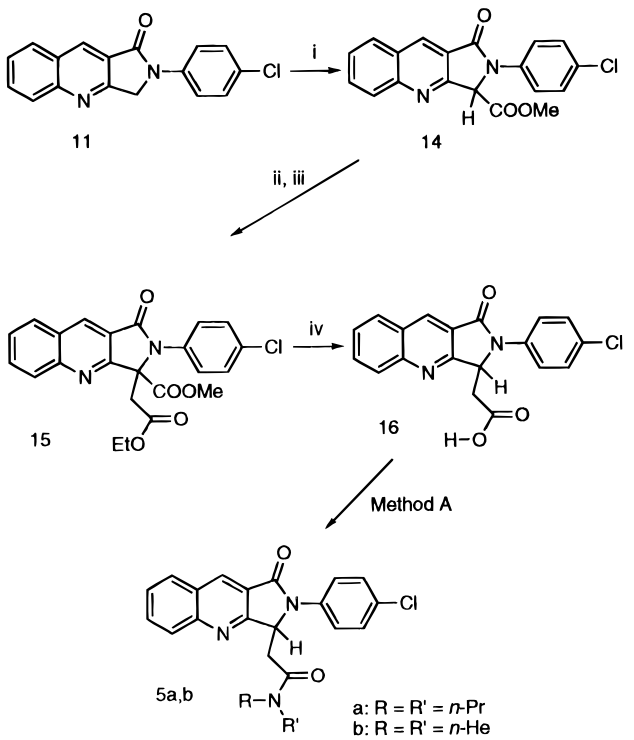

[a] Reagents: (i) NaH, MeOCOOMe, DMF; (ii) DBU, DMF; (iii) $BrCH_2COOEt$/DMF; (iv) NaOH, H_2O, EtOH.

ester groups and spontaneous loss of the carboxyl group attached to the pyrrolidone ring of compound **15** gave the acetic acid derivative **16** (in this behavior, compound **15** is reminiscent of a β-keto ester) which was converted into the corresponding amides **5a**,**b** via mixed anhydrides.

The chemistry developed for the synthesis of compounds **4** and **5** was the same used to obtain compounds **6** and **7** as depicted in Scheme 3. Briefly, commercially available nicotinate **17** was transformed in two steps into the required intermediate **18** which was used in glyoxylic condensation to obtain unsaturated acid **19** or alternatively in a multistep sequence similar to that used for the synthesis of compound **16** to give saturated acid **21**. Both acids **19** and **21** were transformed into the corresponding amides **6a**,**b** and **7a**,**b** via mixed anhydrides.

Results and Discussion

Binding Studies. Initially, the affinities of compounds **4**−**7**, **13**, and **18** for the PBR and CBR in rat cerebral cortex were tested by competition assays against [^{3}H]PK11195 and [^{3}H]flunitrazepam, respectively (see *In Vitro* Binding Assays. Method A). This study revealed that compounds **4a**,**b**,**e**,**f** and **6a** bound with high affinity and selectivity to the PBR (Table 2). In addition, the slopes of the competition curves for compounds **4a**,**e**,**f** were significantly less than 1, suggesting an interaction with multiple PBR-type binding sites. Further analysis of these compounds using competition assays against renal and cortical PBR by means of the selective ligands [^{3}H]Ro5-4864 and [^{3}H]-PK11195 (see *In Vitro* Binding Assays. Method B) revealed that the competition curves for all three

Scheme 3[a]

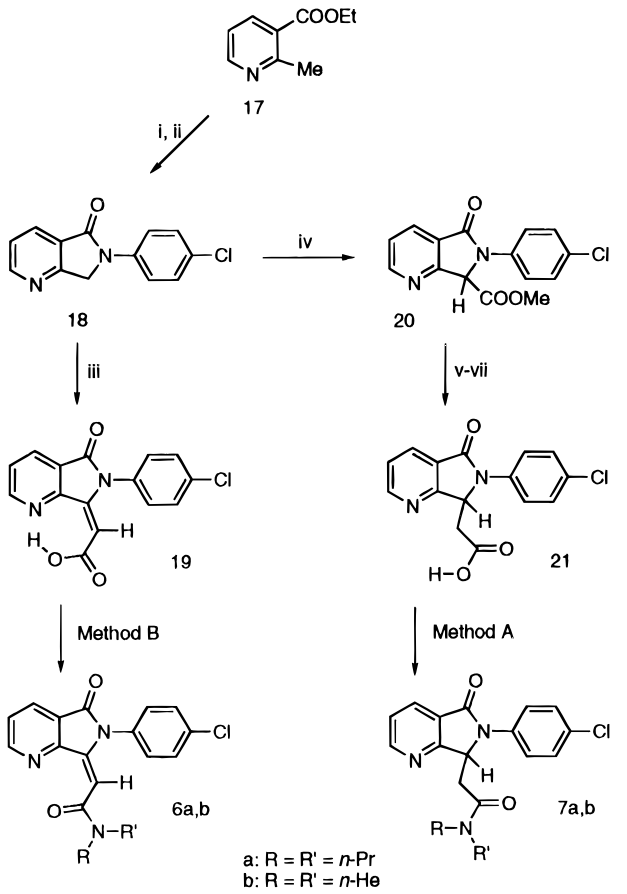

[a] Reagents: (i) NBS, dibenzoyl peroxide, CCl_4; (ii) *p*-$ClC_6H_4NH_2$, EtOH; (iii) $CHOCOOH \cdot H_2O$, Ac_2O, AcOH; (iv) NaH, MeOCOOMe, DMF; (v) DBU, DMF; (vi) $BrCH_2COOEt$, DMF; (vii) NaOH, H_2O, EtOH.

compounds against [^{3}H]PK11195 were biphasic, regardless of the tissue source of PBR (Figure 2), while competition curves against [^{3}H]Ro5-4864 were monophasic. Saturation assays of [^{3}H]PK11195 binding to PBR in renal homogenates were performed in the presence and absence of **4f** (Figure 3). These assays confirmed the existence of two binding sites for [^{3}H]PK11195, in agreement with the competition studies.

While the above studies suggest that [^{3}H]PK11195 binds with equal affinity to two PBR subtypes in the cortex and kidney that can be discriminated by compounds **4a**,**e**,**f**, it is possible that the second site is a nonspecific binding site because of the high level of nonspecific binding associated with [^{3}H]PK11195. Thus, an attempt was made to establish if the second subtype was in fact a nonproteinaceous, non-PBR binding site by measuring specific [^{3}H]PK11195 binding to renal homogenates boiled for 15 min (Figure 2). Under these conditions, all specific binding was eliminated, suggesting that the second site does not reflect nonspecific binding of [^{3}H]PK11195 to membrane lipids.

Structure−Affinity Relationships. From the results summarized in Table 2, it appears that only compound **7a** displays a significant affinity for CBR. This appears to be about 1 order of magnitude lower than that reported for zopiclone, but it is very similar to that reported for compound **3a**.

Interestingly, deletion of acetamide moiety in compound **7a** to give **18** leads to a significant decrease in CBR affinity. This suggests that this structural feature contributes to some extent to the binding process with CBR, but unfortunately the starting CBR affinity of **7a** is not high enough to appreciate the actual importance of this side chain.

The corresponding unsaturated derivative **6a** did not show a CBR affinity, showing at the same time a significant affinity for PBR. The selectivity showed by **6a** seems to be related to the geometry of the side chain. In fact, it is possible to assume for the side chain of **6a** an arrangement near to the mean plane of the molecule as that showed by the X-ray diffraction studies of **4e** (Figure 4), while in compound **7a** the acetamide moiety appeared to be projected out of the mean plane of the molecule by sp^3 hybridization of the pyrrolinone ring methylene.

These findings suggested the existence of a further difference between the interaction model of alpidem with PBR and CBR: The alpidem side chain probably interacts (by its carbonyl dipole) with PBR in a position near to the mean plane, while the interaction with CBR might take place out of the mean plane of the molecule. This would imply that alpidem interacts with PBR and CBR in two different conformations. This hypothesis appears to be very likely owing to the fairly great conformational freedom of alpidem. In this respect compounds **4** and **6** represent conformationally constrained analogues of alpidem lacking a degree of conformational freedom. The high affinity showed by **4a**,**e**,**f** suggests that in these compounds the side chain shows a geometry favorable to the interaction with PBR. When the *E*-geometry at the exocyclic double bond of compound **4a** was inverted to give **13** (*Z*-isomer), all significant PBR affinity was lost confirming the importance of the correct geometry of the acetamide moiety in the interaction with PBR.

Further structure−affinity relationships concern the positive influence (7.2×) of benzocondensation at the *b*-edge of the pyrrolo[3,4-*b*]pyridine nucleus of compounds **6** on PBR affinity. Most probably in this case the benzene ring plays a role similar to that of the 5-chloro substituent in alpidem and compound **2**. Kozikowski[5] and co-workers reported that 5-chloro substitution in compound **2** improved the PBR affinity by about 1 order of magnitude (17×), which indeed appears to be an effect very similar to that induced by benzofusion in the compounds which are the topic of this paper.

Conversely, benzofusion at the *b*-edge of the pyrrolo-[3,4-*b*]pyridine nucleus of compound **7a** appears not to be well tolerated by CBR, since compound **5a** showed no significant affinity for these receptors. As far as the lipophilic amide substituents are concerned, the findings obtained in this study suggest a limited tolerance to the steric hindrance; in fact, relatively small lipophilic groups such as *n*-propyl, *p*-chlorophenyl, and *p*-methoxyphenyl are well accommodated by the receptor, while the bulkier *n*-hexyl groups are not so well tolerated, and finally (quite surprisingly) benzyl groups are not tolerated at all. This minor disagreement with the findings reported by Kozikowski[5] could be related to the greater rigidity of compounds **4** when compared with **2**.

Molecular Modeling. The aim of this part of the work is to assess whether the conclusions offered in the previous section on the basis of the classical medicinal

Table 1. Preparative and Analytical Data of Compounds **4**−**7**

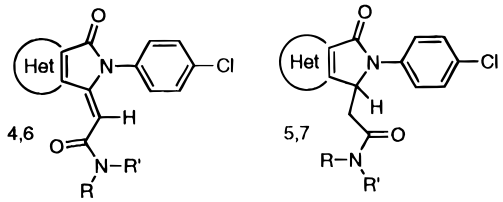

compd	Het[a]	R	R′	method	yield, %	mp, °C (recryst solv)[b]	formula	anal.[c]
4a	Q	*n*-Pr	*n*-Pr	A	67	215−216 (EA)	$C_{25}H_{24}N_3O_2Cl$	CHN
4b	Q	*n*-He	*n*-He	A	62	178−179 (H−EA)	$C_{31}H_{36}N_3O_2Cl$	CHN
4c	Q	Me	CH_2-C_6H_5	B	68	195−196 (H−EA)	$C_{27}H_{20}N_3O_2Cl$	CHN
4d	Q	Et	CH_2-C_6H_5	B	69	186−187 (H−EA)	$C_{28}H_{22}N_3O_2Cl \cdot {}^1/_6H_2O$	CHN
4e	Q	Me	*p*-MeO-C_6H_4	B	60	159−160 (H−EA)	$C_{27}H_{20}N_3O_3Cl$	CHN
4f	Q	Me	*p*-Cl-C_6H_4	B	56	149−151 (H−EA)	$C_{26}H_{17}N_3O_2Cl_2 \cdot {}^1/_3H_2O$	CHN
5a	Q	*n*-Pr	*n*-Pr	A	71	187−188 (H−EA)	$C_{25}H_{26}N_3O_2Cl$	CHN
5b	Q	n-He	*n*-He	A	66	152−153 (H−EA)	$C_{31}H_{38}N_3O_2Cl$	CHN
6a	P	*n*-Pr	*n*-Pr	B	57	116−117 (H−C)	$C_{21}H_{22}N_3O_2Cl$	CHN
6b	P	*n*-He	*n*-He	B	75	111−112 (H)	$C_{27}H_{34}N_3O_2Cl$	CHN
7a	P	*n*-Pr	*n*-Pr	A	69	120−121 (H−EA)	$C_{21}H_{24}N_3O_2Cl$	CHN
7b	P	*n*-He	*n*-He	A	56	81−82 (H)	$C_{27}H_{36}N_3O_2Cl$	CHN

[a] Q, quinoline condensed at *b*-edge; *P*, pyridine condensed at *b*-edge. [b] Recrystallization solvents: EA, ethyl acetate; H, *n*-hexane; C, cyclohexane. [c] Analyses for the elements indicated were within ±0.4% of theoretical values.

Table 2. Affinities of Compounds **4**−**7**, **13**, and **18** for PBR and CBR (IC_{50} (nM) ± SEM)[a]

compd	PBR	CBR
4a	40 ± 13[b]	>1000 (0%)
4b	150 ± 38	>1000 (0%)
4c	>1000 (6%)	NT[c]
4d	>1000 (23%)	NT
4e	1.9 ± 0.2[b]	NT
4f	32 ± 4.7[b]	NT
5a	>1000 (0%)	>1000 (0%)
5b	>1000 (0%)	>1000 (0%)
6a	290 ± 72	>1000 (0%)
6b	33000 ± 2000	>1000 (0%)
7a	>1000	860 ± 230
7b	1600 ± 490	>1000 (0%)
13	>1000 (16%)	NT
18	>1000 (0%)	>1000 (0%)
PK11195	1.8 ± 0.54	
diazepam		5.6 ± 1.3

[a] The IC_{50} values are the means of three experiments performed in duplicate; values in parentheses are the inhibitions at the maximal concentration tested (1000 nM). [b] Compounds **4a**,**e**,**f** displaced [^{3}H]PK11195 in a biphasic manner; linear fitting analysis (single-site model) gave the IC_{50} values reported in the table. [c] NT, not tested.

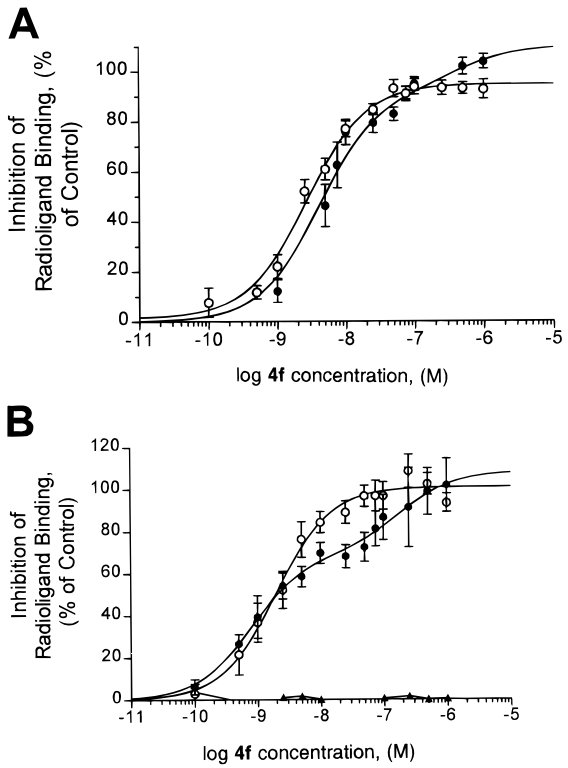

Figure 2. Competition of **4f** with [^{3}H]PK11195 (●) or [^{3}H]-Ro5-4864 (○) for PBR in the brain (panel A) or kidney (panel B). Both radioligand concentrations were approximately 1 nM. Each point represents the summary (mean ± SEM) of data from 8−12 separate observations. Competition assays between **4f** and [^{3}H]Ro5-4864 yielded monophasic curves with IC_{50} values of 2.7 and 2.0 nM (brain and kidney, respectively). In contrast, competition assays between **4f** and [^{3}H]PK11195 revealed the presence of two binding sites, with IC_{50} values in the brain of 4.1 and 400 nM and of 0.8 and 180 nM in the kidney. Competition assays performed between **4f** and [^{3}H]-PK11195 using kidney homogenates boiled for 15 min (△) showed no significant radioligand binding.

chemistry approach can also be substantiated by molecular mechanics calculations. For this purpose we started from the crystal structures as determined by single-crystal X-ray diffraction studies of alpidem[14] and compound **4e** (see X-ray Crystallography section). By taking into account the existing literature on the description of the pharmacophoric elements of the PBR ligands, we chose to adopt the same distance parameters already used by other authors: *d*, distance between the electronegative carboxamide oxygen atom and the centroid of the freely rotating aromatic ring, and *h*, elevation of the carboxamide oxygen atom above the mean plane of the molecule.

As it is possible to observe by comparing Figures 4 and 5, the crystal structure of compound **4e** shows a side chain geometry different from that of alpidem (also in its crystal structure). In fact the values of the distance parameters *d* and *h* in compound **4e** are 6.3 and 1.6 Å, respectively, while the same parameter values of alpidem are 4.6 and 2.3 Å, respectively. The values of the distance parameters *d* and *h* of the crystal structure of compound **4e** appear to be considerably different from the respective values found in the crystal structure of alpidem, but they correlate well with the

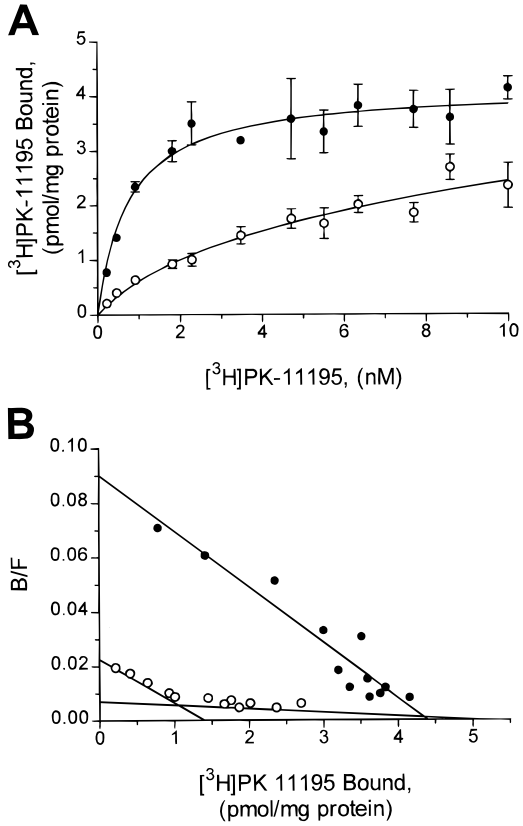

Figure 3. Saturation assays of [^{3}H]PK11195 binding to PBR in kidney homogenates in the presence (○) and absence (●) of 100 nM **4f**. Each point represents the summary (mean ± SEM) of data from 4 (control) and 12 (**4f**) separate observations. Panel A shows the results of the saturation assay presented as a binding isotherm; panel B presents the same data as a Scatchard plot. Lines for the two binding sites observed in the presence of 100 nM **4f** (panel B) were drawn using the values for K_d and B_{max} determined by nonlinear regression. [^{3}H]-PK11195 binds to a single apparent site ($K_d = 1.6 \pm 0.1$ nM, $B_{max} = 4.2 \pm 0.2$ pmol/mg of protein) on renal homogenates in the absence of **4f**. Addition of 100 nM **4f** to the saturation assays results in a shift in radioligand affinity consistent with a competitive inhibition, as well as revealing two binding sites ($K_{d_1} = 2.2 \pm 0.8$ nM, $B_{max_1} = 1.4 \pm 0.2$ pmol/mg of protein; $K_{d_2} = 29 \pm 4.5$ nM, $B_{max_2} = 5.1 \pm 0.5$ pmol/mg of protein).

same distances as determined in the assumed bioactive conformation of PK11195, the typical PBR ligand (d = 6.8 Å, h = 1.1 Å).[11] Furthermore, Lentini and co-workers suggested that the comparison of the most favorable conformational families for some different PBR ligands allowed for a common overlapping zone characterized by d and h values of 6.1 ± 0.2 and 1.4 ± 0.6 Å, respectively.[15] This, also in view of the low flexibility of **4e**, strongly suggests that the crystal conformation of **4e** is probably very similar to the bioactive conformation at PBR sites.

Thus, taking into account the high conformational flexibility of alpidem,[11,14] it can exist in a low-energy conformer close to the crystal conformation of **4e** as showed in Figure 6. This figure also explains the apparent bioisosterism of the replacement of the 5-chlorine atom of compound **2** with a condensed benzo ring (*vide infra* in Results and Discussion section). On the other hand, it is interesting to note that the crystal geometry of alpidem appears to be comparable with that of a low-energy conformer of **7a** which is active at the CBR sites only (Figure 7).

Conclusions

Starting from the high affinity of alpidem for both PBR and CBR, a novel class of potent and selective PBR ligands was designed by comparing the interaction models of alpidem with PBR and CBR. Three members of this class show high affinity and selectivity for PBR and appear to be capable of recognizing two sites labeled by [^{3}H]PK11195. Clearly, the development of these subtype selective ligands based on the alpidem structure will afford investigators new opportunities to establish the range of PBR functions and localization. Finally, the structure−affinity relationships described herein along with the molecular modeling efforts allow the refinement of the original interaction model of alpidem with PBR which can be used to design novel ligands with improved features.

Experimental Section

Melting points were determined in open capillaries on a Büchi 510 apparatus and are uncorrected. Microanalyses were carried out using a Perkin-Elmer 240C elemental analyzer. Merck silica gel 60, 70−230 mesh, was used for column chromatography, and Riedel-de Haen DC-Mikrokarten SI F 37341 were used for TLC. ^{1}H-NMR spectra were recorded with a Bruker AC 200 spectrometer in the solvents indicated (TMS as internal standard); the values of the chemical shifts are expressed in ppm and coupling constants (J) in hertz (Hz). Mass spectra (EI, 70 eV) were recorded on a VG 70-250S spectrometer. IR, NMR spectra, and elemental analyses were performed by the Dipartimento Farmaco Chimico Tecnologico, Università di Siena. Mass spectra were performed by Centro di Analisi e Determinazioni Strutturali, Università di Siena.

General Procedures for the Synthesis of Compounds 4−7. Method A. A mixture of the appropriate carboxylic acid (**12**, **16**, **21**) (0.4 mmol) in anhydrous THF (20 mL) with triethylamine (0.19 mL, 1.4 mmol) was cooled at −10 °C, and isobutyl chloroformate (0.057 mL, 0.44 mmol) was added with stirring under an argon atmosphere. After the mixture stirred for 30 min at −10 °C, the appropriate amine (0.44 mmol) was added and the reaction mixture was allowed to reach room temperature and stirred for 1 h. Then, the reaction mixture was diluted with dichloromethane (20 mL), washed with brine, dried over sodium sulfate, and concentrated under reduced pressure. Recrystallization of the residue from the suitable solvent gave analytically pure amides **4a**,**b**, **5a**,**b**, and **7a**,**b**.

(*E*)-2-(4-Chlorophenyl)-2,3-dihydro-3-[[(*N*,*N*-di-*n*-propylamino)carbonyl]methylene]-1*H*-pyrrolo[3,4-*b*]quinolin-1-one (4a): ^{1}H-NMR ($CDCl_3$) 0.78 (t, J = 7.4, 3H), 1.11 (t, J = 7.4, 3H), 1.42−1.58 (m, 2H), 1.86−2.03 (m, 2H), 3.32 (t, J = 7.4, 2H), 3.53 (t, J = 7.7, 2H), 5.75 (s, 1H), 7.36−7.42 (m, 2H), 7.51−7.57 (m, 2H), 7.65 (t, J = 7.9, 1H), 7.81−7.89 (m, 1H), 8.01 (d, J = 8.0, 1H), 8.17 (d, J = 8.5, 1H), 8.70 (s, 1H).

(*E*)-2-(4-Chlorophenyl)-2,3-dihydro-3-[[(*N*,*N*-di-*n*-hexylamino)carbonyl]methylene]-1*H*-pyrrolo[3,4-*b*]quinolin-1-one (4b): ^{1}H-NMR ($CDCl_3$) 0.77 (t, J = 6.7, 3H), 0.95 (t, J = 6.8, 3H), 1.12−1.61 (m, 14H), 1.87−2.03 (m, 2H), 3.33 (t, J = 7.4, 2H), 3.54 (t, J = 7.8, 2H), 5.75 (s, 1H), 7.36−7.41 (m, 2H), 7.52−7.57 (m, 2H), 7.65 (t, J = 7.4, 1H), 7.85 (t, J = 8.2, 1H), 8.02 (d, J = 7.6, 1H), 8.18 (d, J = 8.4, 1H), 8.70 (s, 1H); MS m/z 517 (M^+, 29).

(±)-2-(4-Chlorophenyl)-2,3-dihydro-3-[[(*N*,*N*-di-*n*-propylamino)carbonyl]methyl]-1*H*-pyrrolo[3,4-*b*]quinolin-1-one (5a): ^{1}H-NMR ($CDCl_3$) 0.72 (t, J = 7.4, 3H), 0.81 (t, J = 7.4, 3H), 1.25−1.51 (m, 4H), 2.90−3.22 (m, 6H), 5.91 (t, J = 4.9, 1H), 7.40−7.45 (m, 2H), 7.60−7.68 (m, 3H), 7.79−7.87 (m, 1H), 8.02 (d, J = 7.4, 1H), 8.16 (d, J = 8.6, 1H), 8.70 (s, 1H).

(±)-2-(4-Chlorophenyl)-2,3-dihydro-3-[[(*N*,*N*-di-*n*-hexylamino)carbonyl]methyl]-1*H*-pyrrolo[3,4-*b*]quinolin-1-one (5b): ^{1}H-NMR ($CDCl_3$) 0.77−0.90 (m, 6H), 1.11−1.33 (m, 16H), 2.89−3.03 (m, 4H), 3.17 (t, J = 7.4, 2H), 5.90 (t, J = 4.8, 1H), 7.39−7.44 (m, 2H), 7.58−7.68 (m, 3H), 7.79−7.87 (m, 1H), 8.02 (d, J = 8.9, 1H), 8.16 (d, J = 8.5, 1H), 8.70 (s, 1H).

Table 3. Characterization of Binding Behavior of Compounds **4a**,**e**,**f** at PBR by Competition Assays

compd	radioligand	tissue	IC_{50_1}, nM	density, $receptor_1$ (% of total)	IC_{50_2}, nM	density, $receptor_2$ (% of total)
4a	[^{3}H]Ro5-4864	cerebral cortex	120 ± 4.7			
	[^{3}H]PK11195		4.9 ± 1.9	82	210 ± 26	18
	[^{3}H]Ro5-4864	kidney	150 ± 18			
	[^{3}H]PK11195		2.7 ± 0.4	82	160 ± 27	18
4e	[^{3}H]Ro5-4864	cerebral cortex	2.3 ± 0.3			
	[^{3}H]PK11195		9.8 ± 0.3	76	320 ± 18	24
	[^{3}H]Ro5-4864	kidney	1.7 ± 0.2			
	[^{3}H]PK11195		0.7 ± 0.3	46	14 ± 2.3	54
4f	[^{3}H]Ro5-4864	cerebral cortex	4.5 ± 0.2			
	[^{3}H]PK11195		2.4 ± 0.3	80	610 ± 160	20
	[^{3}H]Ro5-4864	kidney	2.1 ± 0.1			
	[^{3}H]PK11195		1.1 ± 0.3	71	140 ± 19	29

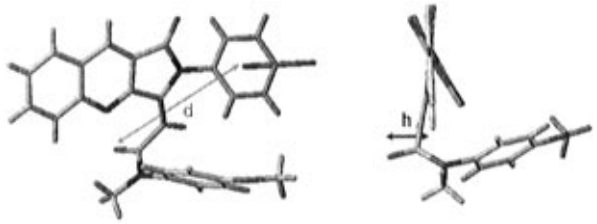

Figure 4. Crystal structure of compound **4e** obtained from X-ray diffraction experiments.

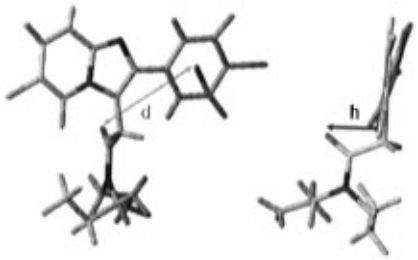

Figure 5. Crystal structure of alpidem built from the crystallographic coordinates obtained from ref 14.

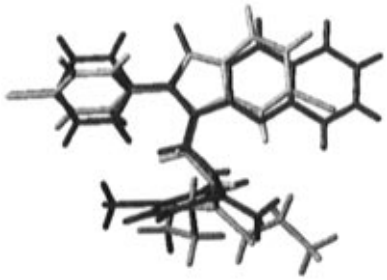

Figure 6. Superposition of a low-energy conformer of alpidem (light) with the solid state conformation of **4e** (dark).

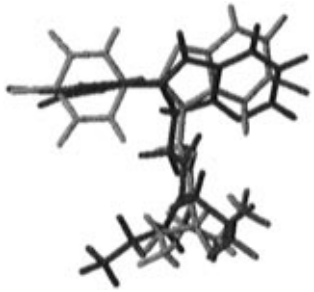

Figure 7. Superposition of the crystal structure of alpidem (light) with a low-energy conformer of **7a** (dark).

(±)-6-(4-Chlorophenyl)-6,7-dihydro-7-[[(*N*,*N*-di-*n*-propylamino)carbonyl]methyl]-5*H*-pyrrolo[3,4-*b*]pyridin-5-one (7a): ^{1}H-NMR ($CDCl_3$) 0.70−0.86 (m, 6H), 1.26−1.47 (m, 4H), 2.76−3.30 (m, 6H), 5.85 (t, J = 5.0, 1H), 7.36−7.47 (m, 3H), 7.57−7.62 (m, 2H), 8.15−8.20 (m, 1H), 8.75−8.79 (m, 1H).

(±)-6-(4-Chlorophenyl)-6,7-dihydro-7-[[(*N*,*N*-di-*n*-hexylamino)carbonyl]methyl]-5*H*-pyrrolo[3,4-*b*]pyridin-5-one (7b): ^{1}H-NMR ($CDCl_3$) 0.80−0.92 (m, 6H), 1.15−1.40 (m, 16H), 2.74−3.33 (m, 6H), 5.85 (t, J = 5.0, 1H), 7.37−7.47 (m, 3H), 7.57−7.62 (m, 2H), 8.15−8.20 (m, 1H), 8.75−8.79 (m, 1H).

Method B. To a mixture of the appropriate carboxylic acid (**12** or **19**) (0.4 mmol) in dichloromethane (10 mL) with triethylamine (0.19 mL, 1.4 mmol) cooled at −10 °C under an argon atmosphere was added isobutyl chloroformate (0.057 mL, 0.44 mmol). The reaction mixture was stirred at −10 °C for 30 min, and then the appropriate amine (0.44 mmol) was added. After the mixture stirred at room temperature for 1 h (48 h for compound **4f**), water (20 mL) was added. The organic layer was washed with water (2 × 20 mL), dried over sodium sulfate, and concentrated under reduced pressure to give amides **4c**−**f** and **6a**,**b**. The amides were recrystallized from the suitable solvent or purified by column chromatography eluting with chloroform−ethyl acetate (8:2) (for compounds **4e**,**f**) and then recrystallized.

(*E*)-3-[[(*N*-Benzylmethylamino)carbonyl]methylene]-2-(4-chlorophenyl)-2,3-dihydro-1*H*-pyrrolo[3,4-*b*]quinolin-1-one (4c):[16] ^{1}H-NMR ($CDCl_3$) 2.99 (s), 3.17 (s), 4.61 (s), 4.87 (s), 5.80 (s), 5.82 (s), 7.22−8.07 (m), 8.25 (d, J = 8.6), 8.72 (s).

(*E*)-3-[[(*N*-Benzylethylamino)carbonyl]methylene]-2-(4-chlorophenyl)-2,3-dihydro-1*H*-pyrrolo[3,4-*b*]quinolin-1-one (4d):[16] ^{1}H-NMR ($CDCl_3$) 1.03 (t, J = 7.3), 1.47 (t, J = 7.3), 3.39 (q, J = 7.2), 3.67 (q, J = 7.2), 4.62 (s), 4.88 (s), 5.71 (s), 5.84 (s), 7.16−7.73 (m), 7.81−7.93 (m), 8.00−8.12 (m), 8.25 (d, J = 8.5), 8.72 (s).

(*E*)-2-(4-Chlorophenyl)-2,3-dihydro-3-[[[*N*-(4-methoxyphenyl)methylamino]carbonyl]methylene]-1*H*-pyrrolo-[3,4-*b*]quinolin-1-one (4e):[16] ^{1}H-NMR ($CDCl_3$) 3.41 (s), 3.55 (s), 3.72 (s), 3.88 (s), 5.60 (s), 5.92 (s), 6.64−6.69 (m), 6.99−7.04 (m), 7.39−7.47 (m), 7.55−7.72 (m), 7.88−8.04 (m), 8.22−8.35 (m), 8.64 (s), 8.74 (s).

(*E*)-2-(4-Chlorophenyl)-3-[[[*N*-(4-chlorophenyl)methylamino]carbonyl]methylene]-2,3-dihydro-1*H*-pyrrolo[3,4-*b*]quinolin-1-one (4f):[16] ^{1}H-NMR ($CDCl_3$) 3.42 (s), 3.57 (s), 5.58 (s), 5.90 (s), 6.64−6.69 (m), 7.02−7.15 (m), 7.45−7.73 (m), 7.85−8.07 (m), 8.30 (d, J = 8.6), 8.65 (s), 8.74 (s).

(*E*)-6-(4-Chlorophenyl)-6,7-dihydro-7-[[*N*,*N*-di-*n*-propylamino)carbonyl]methylene]-5*H*-pyrrolo[3,4-*b*]pyridin-5-one (6a): ^{1}H-NMR ($CDCl_3$) 0.79 (t, J = 7.4, 3H), 1.02 (t, J = 7.4, 3H), 1.39−1.56 (m, 2H), 1.66−1.82 (m, 2H), 3.26 (t, J = 7.5, 2H), 3.42−3.50 (m, 2H), 5.78 (s, 1H), 7.32−7.55 (m, 5H), 8.18 (d, J = 8.3, 1H), 8.80−8.83 (m, 1H).

(*E*)-6-(4-Chlorophenyl)-6,7-dihydro-7-[[*N*,*N*-di-*n*-hexylamino)carbonyl]methylene]-5*H*-pyrrolo[3,4-*b*]pyridin-5-one (6b): ^{1}H-NMR ($CDCl_3$) 0.81 (t, J = 6.3, 3H), 0.91 (t, J = 6.5, 3H), 1.12−1.54 (m, 14H), 1.67−1.82 (m, 2H), 3.27 (t, J = 7.4, 2H), 3.49 (t, J = 7.5, 2H), 5.77 (s, 1H), 7.31−7.54 (m, 5H), 8.16−8.20 (m, 1H), 8.80−8.83 (m, 1H).

Ethyl 4-Chloro-3-anilinocrotonate (9). In a 100 mL flask, attached to a Dean−Stark constant water separator which was connected to a reflux condenser, 4.66 g (50.0 mmol) of aniline (**8**), 6.82 mL (50.0 mmol) of ethyl 4-chloroacetoacetate, 50 mL of benzene, and 5 mL of glacial acetic acid were placed. The flask was heated to reflux for 2 h. The solvent was then distilled under reduced pressure; toluene (10 mL)

was added and distilled under reduced pressure (the operation was repeated twice). The residue was diluted with chloroform−light petroleum ether (1:1, 50 mL), and the solid was filtered off. The filtrate was concentrated under reduced pressure. Purification by culumn chromatography of the residue eluting with chloroform−light petroleum ether (1:1) afforded **9** (4.8 g, yield 40%) as an oil which was used in the next step without further handling: ^{1}H-NMR ($CDCl_3$) 1.30 (t, J = 6.9, 3H), 4.09 (s, 2H), 4.18 (q, J = 6.9, 2H), 5.01 (s, 1H), 7.16−7.42 (m, 5H), 10.07 (br s, 1H).

Ethyl 2-(Chloromethyl)-3-quinolinecarboxylate (10). To 1.7 mL (22.0 mmol) of anhydrous DMF cooled at 0−5 °C was slowly added phosphorus oxychloride (6.0 mL, 65.5 mmol). The resultant reagent was stirred at room temperature for 30 min and then cooled to 0−5 °C. A solution of **9** (4.8 g, 20.0 mmol) in chloroform (40 mL) was added, and the reaction mixture was heated to reflux for 45 min. Then, the cooled reaction mixture was poured into saturated sodium bicarbonate solution and extracted with chloroform (3 × 20 mL). The combined organic extracts were washed with saturated sodium bicarbonate solution (2 × 20 mL), dried over sodium sulfate, and concentrated under reduced pressure. The residue was recrystallized from ethanol to give **10** (3.2 g, yield 64%) as white prisms. An analytical sample melted at 120−121 °C: ^{1}H-NMR ($CDCl_3$) 1.48 (t, J = 7.1, 3H), 4.50 (q, J = 7.2, 2H), 5.28 (s, 2H), 7.62 (t, J = 7.4, 1H), 7.79−7.94 (m, 2H), 8.13 (d, J = 8.4, 1H), 8.82 (s, 1H). Anal. ($C_{13}H_{12}NO_2Cl$) C, H, N.

2-(4-Chlorophenyl)-2,3-dihydro-1*H*-pyrrolo[3,4-*b*]quinolin-1-one (11). A mixture of **10** (2.3 g, 9.2 mmol) in ethanol (60 mL) with 4-chloroaniline (3.5 g, 27.4 mmol) was refluxed for 53 h. The reaction mixture was allowed to reach room temperature, and the crystals formed were collected by filtration, washed with cold ethanol and then with light petroleum ether, and finally dried under reduced pressure. Thus, 2.5 g (yield 92%) of pure **11** was obtained as white needles. An analytical sample recrystallized from ethanol−DMF melted at 268−270 °C: ^{1}H-NMR ($CDCl_3$) 5.03 (s, 2H), 7.41−7.46 (m, 2H), 7.66 (t, J = 7.3, 1H), 7.83−7.92 (m, 3H), 8.04 (d, J = 8.3, 1H), 8.19 (d, J = 8.5, 1H), 8.71 (s, 1H). Anal. ($C_{17}H_{11}N_2OCl$) C, H, N.

(*E*)-3-(Carboxymethylene)-2-(4-chlorophenyl)-2,3-dihydro-1*H*-pyrrolo[3,4-*b*]quinolin-1-one (12). A mixture of **11** (0.3 g, 1.02 mmol) in glacial acetic acid (5 mL) and acetic anhydride (5 mL) with glyoxylic acid monohydrate (0.3 g, 3.26 mmol) was heated at 110 °C for 5 h under nitrogen atmosphere. Then 0.3 g of glyoxylic acid monohydrate was added, and the mixture was stirred at 110 °C for an additional 1 h. Afterward the cooled reaction mixture was poured into ice−water and allowed to stand at room temperature overnight. The precipitate was extracted with chloroform (2 × 50 mL), and the organic layer was extracted with diluted NaOH (pH 9−10) (2 × 60 mL). The organic layer was discarded, and the acqueous phase was acidified (pH 4−5) with 3 N HCl and extracted with chloroform (3 × 20 mL). The combined extracts were dried over sodium sulfate and concentrated under reduced pressure to give crude **12** which was purified by column chromatography eluting with chloroform−ethyl acetate (8:2) to give 0.21 g of pure **12** as white crystals (yield 59%). An analytical sample recrystallized from ethanol−chloroform melted at 272−273 °C: ^{1}H-NMR ($CDCl_3$) 5.89 (s, 1H), 7.27−7.35 (m, 2H), 7.54−7.61 (m, 2H), 7.86 (t, J = 8.0, 1H), 8.03−8.11 (m, 1H), 8.19 (d, J = 8.4, 1H), 8.32 (d, J = 8.5, 1H), 8.96 (s, 1H), 16.13 (s, 1H). Anal. ($C_{19}H_{11}N_2O_3Cl\cdot{}^1/_3H_2O$) C, H, N.

(*Z*)-2-(4-Chlorophenyl)-2,3-dihydro-3-[[(*N*,*N*-di-*n*-propylamino)carbonyl]methylene]-1*H*-pyrrolo[3,4-*b*]quinolin-1-one (13). A mixture of **12** (0.094 g, 0.27 mmol) in thionyl chloride (3 mL, 41 mmol) was stirred at room temperature for 1.5 h. The excess of thionyl chloride was removed under reduced pressure, and toluene (15 mL) was added. To the resulting suspension, cooled at 0−5 °C, was added *N*,*N*-di-*n*-propylamine (1.0 mL, 7.29 mmol). After stirring at room temperature for 15 min, the mixture was diluted with dichloromethane (30 mL), washed with water (3 × 20 mL), dried, and finally concentrated under reduced pressure. Purification of the residue by chromatography, eluting with chloroform−ethyl acetate (8:2), gave first 0.017 g (yield 14%) of pure **4a** and then 0.065 g (yield 55%) of pure **13** as a white solid. Recrystallization of **13** from *n*-hexane−ethyl acetate gave an analytical sample melting at 172−173 °C: ^{1}H-NMR ($CDCl_3$) 0.80 (t, J = 7.3, 3H), 0.94 (t, J = 7.4, 3H), 1.12−1.24 (m, 2H), 1.51−1.67 (m, 2H), 2.91−2.99 (m, 2H), 3.24 (t, J = 7.5, 2H), 6.83 (s, 1H), 7.28−7.34 (m, 2H), 7.41−7.46 (m, 2H), 7.67 (t, J = 8.0, 1H), 7.85−7.93 (m, 1H), 8.05 (d, J = 9.0, 1H), 8.26 (d, J = 8.5, 1H), 8.72 (s, 1H). Anal. ($C_{25}H_{24}N_3O_2Cl$) C, H, N.

(±)-2-(4-Chlorophenyl)-2,3-dihydro-3-(methoxycarbonyl)-1*H*-pyrrolo[3,4-*b*]quinolin-1-one (14). A mixture of **11** (1.0 g, 3.4 mmol) with sodium hydride (0.24 g, 10.0 mmol) in dimethyl carbonate (12 mL, 142.4 mmol) and anhydrous DMF (4 mL) was gently refluxed for 30 min under argon atmosphere. Then, the dark violet mixture was poured into ice−water and acidified with 0.6 N HCl. The precipitate was collected by filtration, washed with water and then with diethyl ether, and dried under reduced pressure to give 1.1 g of pure **14** as a white solid (yield 92%). An analytical sample recrystallized from ethyl acetate melted at 243−244 °C: ^{1}H-NMR ($CDCl_3$) 3.78 (s, 3H), 5.90 (s, 1H), 7.40−7.45 (m, 2H), 7.65−7.76 (m, 3H), 7.90 (t, J = 8.1, 1H), 8.05 (d, J = 8.0, 1H), 8.27 (d, J = 8.5, 1H), 8.74 (s, 1H). Anal. ($C_{19}H_{13}N_2O_3Cl$) C, H, N.

(±)-2-(4-Chlorophenyl)-2,3-dihydro-3-[(ethoxycarbonyl)methyl]-3-(methoxycarbonyl)-1*H*-pyrrolo[3,4-*b*]quinolin-1-one (15). To a solution of **14** (0.1 g, 0.28 mmol) in anhydrous DMF (15 mL) under an argon atmosphere was slowly added DBU (0.45 mL, 3.0 mmol) under stirring at room temperature. After 10 min at room temperature to the dark blue-colored solution was slowly added ethyl bromoacetate (0.4 mL, 3.6 mmol) up to the complete decoloration of the solution. The mixture was stirred for 10 min at room temperature and then poured into ice−water and extracted with dichloromethane (4 × 20 mL). The combined extracts were washed with water (5 × 50 mL), dried over sodium sulfate, and concentrated under reduced pressure. Purification of the residue by column chromatography, eluting with chloroform−ethyl acetate (8:2), gave **15** (0.11 g, yield 90%) as a thick oil which was characterized only by its ^{1}H-NMR spectrum: ^{1}H-NMR ($CDCl_3$) 0.92 (t, J = 7.4, 3H), 3.29 (d, J = 17.7, 1H), 3.72 (s, 3H), 3.76−3.96 (m, 3H), 7.28−7.34 (m, 2H), 7.39−7.46 (m, 2H), 7.66 (t, J = 7.2, 1H), 7.82−7.90 (m, 1H), 8.05 (d, J = 7.7, 1H), 8.21 (d, J = 8.5, 1H), 8.74 (s, 1H).

(±)-3-(Carboxymethyl)-2-(4-chlorophenyl)-2,3-dihydro-1*H*-pyrrolo[3,4-*b*]quinolin-1-one (16). To a solution of **15** (0.55 g, 1.25 mmol) in ethanol (35 mL) was added 3 N sodium hydroxide solution (15 mL, 45.0 mmol), and the resulting mixture was stirred at room temperature for 2 h. Then, the organic solvent was removed under reduced pressure, and water (50 mL) was added. The basic solution was extracted with dichloromethane (2 × 15 mL), and the organic extracts were discarded, while the aqueous solution was acidified with 3 N HCl. The precipitate was collected by filtration and dried to give crude **16** which was purified by recrystallization from ethanol−chloroform (0.36 g, yield 82%). An analytical sample melted at 280−282 °C dec: ^{1}H-NMR (DMSO-d_6) 2.86−3.18 (m, 2H), 5.84 (t, J = 4.1, 1H), 7.56 (d, J = 8.7, 2H), 7.69−7.74 (m, 3H), 7.93 (t, J = 7.5, 1H), 8.15 (d, J = 8.5, 1H), 8.25 (d, J = 8.2, 1H), 8.88 (s, 1H), 12.17 (s, 1H). Anal. ($C_{19}H_{13}N_2O_3Cl$) C, H, N.

6-(4-Chlorophenyl)-6,7-dihydro-5*H*-pyrrolo[3,4-*b*]pyridin-5-one (18). A mixture of ethyl 2-methylnicotinate (**17**) (1.6 mL, 10.4 mmol) in carbon tetrachloride (50 mL) with NBS (1.7 g, 9.6 mmol) and 75% dibenzoyl peroxide (0.2 g, 0.6 mmol) was refluxed for 17 h. Then, the cooled reaction mixture was filtered, and the filtrate was concentrated under reduced pressure. The residue was dissolved in ethanol (45 mL), and 4-chloroaniline (4.0 g, 31.3 mmol) was added. After refluxing for 3 days, the reaction mixture was allowed to reach room temperature and a solid crystallized on standing. The crystals were collected by filtration, washed with cold ethanol and then with light petroleum ether, and finally dried to give pure **18** (0.9 g, yield 35%). An analytical sample recrystallized from ethanol melted at 198−199 °C: ^{1}H-NMR ($CDCl_3$) 4.90 (s, 2H), 7.38−7.49 (m, 3H), 7.79−7.86 (m, 2H), 8.17−8.21 (m, 1H), 8.78−8.81 (m, 1H). Anal. ($C_{13}H_9N_2OCl$) C, H, N.

(*E*)-7-(Carboxymethylene)-6-(4-chlorophenyl)-6,7-dihydro-5*H*-pyrrolo[3,4-*b*]pyridin-5-one (19). A mixture of **18** (0.3 g, 1.23 mmol) in glacial acetic acid (5 mL) and acetic anhydride (5 mL) with glyoxylic acid monohydrate (0.3 g, 3.26 mmol) was refluxed for 3 h under a nitrogen atmosphere. Then the cooled reaction mixture was poured into ice−water and allowed to stand at room temperature ovenight. The dark precipitate was collected by filtration, washed with water, dried, and purified by column chromatography eluting with chloroform−ethyl acetate (8:2) to give pure **19** (0.22 g, yield 59%). An analytical sample recrystallized from ethanol−chloroform melted at 278−279 °C dec: ^{1}H-NMR ($CDCl_3$) 5.86 (s, 1H), 7.25−7.29 (m, 2H), 7.53−7.58 (m, 2H), 7.76−7.83 (m, 1H), 8.46 (d, J = 7.9, 1H), 8.89−8.93 (m, 1H), 15.51 (s, 1H). Anal. ($C_{15}H_9N_2O_3Cl$) C, H, N.

(±)-6-(4-Chlorophenyl)-6,7-dihydro-7-(methoxycarbonyl)-5*H*-pyrrolo[3,4-*b*]pyridin-5-one (20). Starting from **18** (0.8 g, 3.27 mmol) the title compound **20** was prepared following the procedure described above for **14**. Pure **20** was obtained as a white solid (0.82 g, yield 83%). An analytical sample was obtained from ethyl acetate as white needles melting at 223−224 °C dec: ^{1}H-NMR ($CDCl_3$) 3.77 (s, 3H), 5.78 (s, 1H), 7.38−7.43 (m, 2H), 7.49−7.56 (m, 1H), 7.64−7.69 (m, 2H), 8.20−8.25 (m, 1H), 8.80−8.83 (m, 1H). Anal. ($C_{15}H_{11}N_2O_3Cl$) C, H, N.

(±)-7-(Carboxymethyl)-6-(4-chlorophenyl)-6,7-dihydro-5*H*-pyrrolo[3,4-*b*]pyridin-5-one (21). To a solution of **20** (0.5 g, 1.65 mmol) in anhydrous DMF (35 mL) under an argon atmosphere was added DBU (2.4 mL, 16.05 mmol) at room temperature. After stirring at the same temperature for 10 min, to the resulting red solution was slowly added ethyl bromoacetate (1.6 mL, 14.43 mmol) up to the complete decoloration of the solution. The mixture was stirred for 10 min at room temperature and then poured into ice−water and extracted with dichloromethane (4 × 25 mL). The organic layer was thoroughly washed with water (5 × 60 mL), dried over sodium sulfate, and concentrated under reduced pressure. The residue was dissolved in ethanol (35 mL), and a 3 N sodium hydroxide solution (15 mL, 45.0 mmol) was added under vigorous stirring at room temperature. After 2 h at the same temperature, the organic solvent was removed under reduced pressure and water (50 mL) was added. The basic solution was extracted with dichloromethane (2 × 15 mL); the combined organic extracts were discarded, and the aqueous solution was acidified with 3 N HCl. The precipitate was collected by filtration, washed with water, and dried to give pure **21** (0.29 g, yield 58%). An analytical sample obtained from ethyl acetate melted at 196−198 °C: ^{1}H-NMR (DMSO-d_6) 2.71−3.01 (m, 2H), 5.70 (t, J = 4.5, 1H), 7.50−7.67 (m, 5H), 8.17 (d, J = 8.1, 1H), 8.80 (d, J = 5.0, 1H), 12.15 (s, 1H). Anal. ($C_{15}H_{11}N_2O_3Cl$) C, H, N.

X-ray Crystallography. A single crystal of **4e** was submitted to X-ray data collection on a Siemens P4 four-circle diffractometer with graphite-monochromated Mo Kα radiation. The $\omega/2\theta$ scan technique was used. The structure was solved by direct methods. The refinement was carried out by full-matrix anisotropic least-squares on F for all non-H atoms by minimizing the function $\sum w(|F_o| - |F_c|)^2$. Atomic scattering factors including f' and f'' were taken from ref 17. Structure solution, analysis, and refinement were carried out by using the SHELXTL PC package.[17]

4e: $C_{27}H_{20}N_3O_3Cl$ (MW 469.9), a pale-yellow single crystal, dimensions 0.3 × 0.3 × 0.08 mm, was used for data collection; orthorhombic; space group *Pbca*; a = 19.613(4) Å, b = 10.456(2) Å, c = 22.118(4) Å, V = 4536(2) Å^3, Z = 8, D_c = 1.38 g/cm^3; 2961 independent reflections (R_{int} = 0.016) were collected at 22 °C, of which 1985 were observed with $F > 3\sigma(F)$. No absorption correction was applied. The final refinement converged to R = 0.047 and R_w = 0.036. Minimum and maximum heights in last $\Delta\rho$ map of −0.23 and 0.21 eÅ^{-3}. Full crystallographic details will be given elsewhere.

Molecular Modeling and Computational Procedures. The entire molecular modeling study was performed using the Sybyl[18] software package installed on a SGI Indy 4400 workstation. Molecules were built up either using X-ray coordinates (alpidem, **4e**) or de novo (**7a**) starting from geometry-optimized fragments (Tripos fragment library as implemented in Sybyl 6.1) and subsequent minimization of the potential energy to the closest local minimum using the standard Tripos force field.[19] Charges were calculate using the method of Gasteiger and Marsili.[20] Molecular dynamics simulation runs were performed using the following protocol: 10 ps of thermal equilibration at 1000 K, 200 ps simulation at 300 K; time step, 1 fs; temperature-coupling factor, 10 fs; nonbonded reset frequency, 25 fs; momentum removal frequency, 25 fs; starting velocity, Boltzman.

Conformers were saved every 100 fs from the simulation period at 300 K resulting in a total number of 2000 structures. For conformer classification, two geometric features were defined and evaluated as follows: (i) a centroid (dummy atom located in the rms distance of all carbon atoms of the phenyl substituent) and (ii) a plane (defined by rms of all atoms of the fused aromatic system). The distance between the centroid and the amide oxygen atom and the height of the latter above the plane were measured in all conformers recorded.

***In Vitro* Binding Assays. Method A.** Male CRL:CD(SD)-BR-COBS rats were killed by decapitation. Their brains were rapidly dissected into the various areas and stored at −80 °C until the day of assay.

CBR. The synaptosomal membrane of rat cerebral cortex was prepared according to Mohler and Okada.[21] Rat cerebral cortices were homogenized (Polytron PTA 10TS) in 22 vol of 0.32 M sucrose at 0 °C (3 × 20 s). The homogenate was centrifuged for 10 min at 1000*g* at 4 °C, and the supernatant was recentrifuged for 10 min at 20000*g* (Beckman model J2-21 refrigerated centrifuge). The pellet was resuspended in 22 vol of phosphate buffer (25 mM, pH 7.4) and centrifuged as before. The final pellet was resuspended in the incubation buffer (phosphate, 25 mM, pH 7.4) just before the binding assay.

[^{3}H]Flunitrazepam (specific activity 79.6 Ci/mmol; NEN) binding was assayed in a final incubation volume of 1.0 mL, consisting of 0.5 mL of membrane suspension (2.5 mg of tissue, wet weight), 0.1 mL of [^{3}H]flunitrazepam (final concentration = 1 nM), 0.1 mL of displacing agent (dissolved in 5% DMSO) or solvent, and 0.3 mL of the incubation buffer.

Incubations (20 min at room temperature) were terminated by rapid filtration under vacuum through GF/B filters which were then washed with 13.5 mL (3 × 4.5 mL) of phosphate buffer (25 mM, pH 7.4) using a Brandel M-24R cell harvester. Nonspecific binding was defined as nondisplaceable binding in the presence of diazepam (10 μM). Blank experiments were carried out to determine the effect of the solvent (5% DMSO) on the binding.

PBR. The binding assays were performed as described in ref 22. The frozen cortices were homogenized in 50 vol of ice-cold phosphate buffer, 50 mM, pH 7.4, using a Polytron PTA 10TS (3 × 20 s). The homogenate was centrifuged for 10 min at 1000*g* at 4 °C, and the supernatant was recentrifuged at 50000*g* for 10 min (Beckman model J2-21 refrigerated centrifuge). Each pellet was washed another three times by resuspension in the same volume of fresh buffer and centrifuged again at 50000*g* for 10 min without intermediate incubations. The pellet obtained was finally resuspended in phosphate (50 mM, pH 7.4) incubation buffer just before the binding assay.

[^{3}H]PK11195 (specific activity 85.5 Ci/mmol; NEN) binding was assayed in a final incubation volume of 1.0 mL, consisting of 0.5 mL of membrane suspension, 0.1 mL of [^{3}H]ligand, and 0.1 mL of displacing agent or solvent. Tissue concentration and [^{3}H]PK11195 final concentration were 2.3 mg of tissue/sample and 1 nM, respectively.

Incubations (120 min at 4 °C) were stopped by rapid filtration under vacuum through GF/B filters which were then washed with 12 mL (3 × 4 mL) of ice-cold phosphate buffer (50 mM, pH 7.4) using a Brandel M-24R cell harvester. Nonspecific binding was assayed in the presence of PK11195 (10 μM).

Dried filters were immersed in vials containing 10 mL of Filter Count (Packard) liquid scintillation cocktail for the measurement of trapped radioactivity with a Packard Tri-Carb 300C liquid scintillation spectrometer at a counting efficiency of about 60%. The concentration of the test compounds that

inhibited [^{3}H]ligand binding by 50% (IC_{50}) was determined by log−probit analysis with six concentrations of the displacers, each performed in duplicate.

Method B. [^{3}H]Ro5-4864 or [^{3}H]PK11195 binding to PBR in rat brain and kidney was performed as previously described.[23] Rats were sacrificed according to AAALAC guidelines and the brain and a kidney removed and placed into ice-cold 0.32 M sucrose. The brain (1.5−2 g) and a section of kidney (100−150 mg) were homogenized in 50 vol of 50 mM Tris-HCl (pH 7.4, 0−4 °C) using a Polytron (Brinkmann Instruments, Westbury, NY). The homogenates were centrifuged once at 20000*g* for 20 min, and the pellet was retained and resuspended in 100 (brain) or 400 (kidney) vol of 50 mM Tris-HCl buffer. An aliquot of tissue suspension (250 μL of brain ≈ 200 μg of protein; 50 μL of kidney ≈ 20 μg of protein) was added to each assay tube in addition to 50 μL of [^{3}H]Ro5-4864 (specific activity 86.9 Ci/mmol) or [^{3}H]PK11195 (specific activity 83.5 Ci/mmol; DuPont/New England Nuclear, Boston, MA). The final concentrations used of both radioligands were 1 nM for competition assays and 0.25−10 nM for saturation assays.

Nonspecific binding was determined using either unlabeled PK11195 or Ro5-4864 (50 μM, final concentration 10 μM) for [^{3}H]Ro5-4864 or [^{3}H]PK11195 binding, respectively. Sufficient buffer was added to bring the final volume to 500 μL. All assays were performed in duplicate. The assay was initiated by the addition of tissue and terminated after 60 min of incubation at 0−4 °C ([^{3}H]Ro5-4864) or at room temperature ([^{3}H]PK11195) by rapid filtration over no. 32 glass fiber filters (Schleicher & Schuell, Keene, NH) using a Brandel M-24R filtering manifold (Brandel Instruments, Gaithersburg, MD). The samples were washed with two 5 mL aliquots of 50 mM Tris-HCl buffer (pH 7.4, 0−4 °C). The radioactivity retained by the filters was measured by an LS 5801 liquid scintillation spectrometer (Beckman Instruments, Fullerton, CA) using 4 mL of scintillation cocktail (Cytoscint, ICN Biomedical, Aurora, OH). Protein concentrations were determined using the bicinchoninic acid technique (Pierce Chemicals, Rockland, IL).

Sigmoidal competition and hyperbolic saturation curves were fit to the appropriate data using nonlinear regression binding techniques. The goodness-of-fit of curves modeling single and multiple binding sites to the data was assessed using the *F*-test. All analyses were performed using Prism2 (GraphPad Softaware, San Diego, CA).

Acknowledgment. The authors are grateful to Dr. Jean Jacques Bourguignon for his collaboration. This work was financially supported by Italian MURST (60% and 40% funds).

References

(1) Fryer, R. I. Ligand Interaction at the Benzodiazepine Receptor. In *Comprehensive Medicinal Chemistry*; Hansch, C., Sammes, P. G., Taylor, J. B., Eds.; C. A. Ramsden Pergamon Press: New York, 1990; Vol. 3, Chapter 12.8, pp 539−566 and references cited therein.

(2) (a) Braestrup, C.; Squires, R. F. Specific Benzodiazepine Receptors in Rat Brain Characterized By High Affinity [^{3}H]Diazepam Binding. *Proc. Natl. Acad. Sci. U.S.A.* **1977**, *74*, 3805−3809. (b) Taniguchi, T.; Wang, J. K. T.; Spector, S. [^{3}H]Diazepam Binding Sites on Rat Heart and Kidney. *Biochem. Pharmacol.* **1982**, *31*, 589−590.

(3) Gavish, M.; Katz, Y.; Bar-Ami, S.; Weizman, R. Biochemical, Physiological, and Pathological Aspects of the Peripheral Benzodiazepine Receptor. *J. Neurochem.* **1992**, *58*, 1589−1601.

(4) *Peripheral Benzodiazepine Receptors*; Giesen-Crouse, E., Ed.; Academic Press: London, 1993.

(5) Kozikowski, A. P.; Ma, D.; Brewer, J.; Sun, S.; Costa, E.; Romeo, E.; Guidotti, A. Chemistry, Binding Affinities, and Behavioral Properties of a New Class of "Antineophobic" Mitochondrial DBI Receptor Complex (mDRC) Ligands. *J. Med. Chem.* **1993**, *36*, 2908−2920.

(6) (a) Bourguignon, J. J. Endogenous and Synthetic Ligand of Mitochondrial Benzodiazepine Receptors: Structure-Affinity Relationships. In *Peripheral Benzodiazepine Receptors*; Giesen-Crouse, E., Ed.; Academic Press: London, 1993; pp 59−85. (b) Costa, E.; Romeo, E.; Auta, J.; Papadopoulos, V.; Kozikowski, A. P.; Guidotti, A. Is There a Pharmacology of Brain Steroidogenesis? In *Neurosteroid and Brain Function, Fidia Research Fundation Symposium Series*; Costa, E., Paul, S. M., Eds.; Thieme Medical Publisher, Inc.: New York, 1991; pp 171−176. (c) Romeo, E.; Auta, J.; Kozikowski, A. P.; Ma, D.; Papadopoulos, V.; Puia, G.; Costa, E.; Guidotti, A. 2-Aryl-3-Indoleacetamides (FGIN-1): A New Class of Potent and Specific Ligands for the Mitochondrial DBI Receptor (MDR). *J. Pharmacol. Exp. Ther.* **1992**, *262*, 971−978. (d) Kozikowski, A. P.; Ma, D.; Romeo, E.; Auta, J.; Papadopoulos, V.; Puia, G.; Costa, E.; Guidotti, A. Synthesis of (2-Arylindol-3-yl)acetamides as Probes of Mitochondrial Steroidogenesis - A New Mechanism for $GABA_A$ Receptor Modulation. *Angew. Chem., Int. Ed. Engl.* **1992**, *31*, 1060−1062.

(7) Tebib, S.; Bourguignon, J. J.; Wermuth, C. G. The Active Analogue Approach Applied to the Pharmachophore Identification of Benzodiazepine Receptor Ligands. *J. Comput.-Aided Mol. Des.* **1987**, *1*, 153−170 and references cited therein.

(8) Tomczuk, B. E.; Taylor, C. R.; Moses, L. M.; Sutherland, D. B.; Lo, Y. S.; Johnson, D. N.; Kinnier, W. B.; Kilpatrick, B. F. 2-Phenyl-3H- imidazo[4,5-b]pyridine-3-acetamides as Non-Benzodiazepine Anticonvulsants and Anxiolytics. *J. Med. Chem.* **1991**, *34*, 2993−3006.

(9) (a) Anzini, M.; Cappelli, A.; Vomero, S.; Giorgi, G.; Langer, T.; Hamon, M.; Nacera, M.; Emerit, B. M.; Cagnotto, A.; Skorupska, M.; Mennini, T.; Pinto, J. C. Novel Potent and Selective 5-HT_3 Receptor Antagonists Based on Arylpiperazine Skeleton: Synthesis, Structure, Biological Activity and CoMFA Studies. *J. Med. Chem.* **1995**, *38*, 2692−2704. (b) Cappelli, A.; Anzini, M.; Vomero, S.; Menziani, M. C.; De Benedetti, P. G.; Sbacchi, M.; Mennuni, L. Synthesis, Biological Evaluation, and Quantitative Receptor Docking Simulation of 2-Acylaminoethyl-1,4-benzodiazepines as Novel Tifluadom-Like Ligands with High Affinity and Selectivity for κ-Opioid Receptors. *J. Med. Chem.* **1996**, *39*, 860−872.

(10) Borea, P. A.; Gilli, G.; Bertolasi, V.; Ferretti, V. Stereochemical Features Controlling Binding and Intrinsic Activity Properties of Benzodiazepine-Receptor Ligands. *Mol. Pharmacol.* **1987**, *31*, 334−344.

(11) Georges, G.; Vercauteren, D. P.; Vanderveken, D. J.; Horion, R.; Evrard, G.; Fripiat, J. G.; Andre, J. M.; Durant, F. Structural and Electronic Analysis of Peripheral Benzodiazepine Ligands: Description of the Pharmacophoric Elements for Their Receptor. *Int. J. Quant. Chem. Quant. Biol. Symp.* **1990**, *17*, 1−25.

(12) Adams, D. R.; Dominguez, J. N.; Perez, J. A. Synthesis of Quinolines by Reaction of Anilinobutenoates with Vilsmeier Reagent. *Tetrahedron Lett.* **1983**, *24*, 517−518.

(13) Anzini, M.; Cappelli A.; Vomero, S. Synthesis of 2-Substituted 2,3-dihydro-9-phenyl-1H-pyrrolo[3,4-b]quinolin-3-ones as Potential Peripheral Benzodiazepine Receptor Ligands. *Heterocycles* **1994**, *38*, 103−111.

(14) Georges, G. J.; Vercauteren, D. P.; Evrard, G. H.; Durant, F. V.; George, P. G.; Wick, A. E. Characterization of the Physico-Chemical Properties of the Imidazopyridine derivative Alpidem. Comparison with Zolpidem. *Eur. J. Med. Chem.* **1993**, *28*, 323−335.

(15) Lentini, G.; Bourguignon, J. J.; Wermuth, C. G. Ligands of the Peripheral-Type Benzodiazepine Binding Sites (PBS): Structure-Activity Relationships and Computer-Aided Conformational Analysis. In *QSAR: Rational Approaches to the Design of Bioactive Compounds*; Silipo, C., Vittoria, A., Eds.; Elsevier Science Publishers B.V.: Amsterdam, 1991; pp 257−260.

(16) Since the amide nitrogen of this compound bears two different substituents, its ^{1}H-NMR spectrum shows the presence of two different rotamers in equilibrium. For the sake of simplification the integral intensities are not given.

(17) SHELXTL PC, Siemens Analytical X-Ray Instruments, Inc., Madison, WI; Rel. 4.1, 1990.

(18) SYBYL 6.1, Tripos Assoc., 1699 S. Hanley Rd., Suite 303, St. Louis, MO 63144.

(19) Clark, M.; Cramer, R. D., III; Van Opdenbosch, N. Validation of the General Purpose TRIPOS 5.2 Force Field. *J. Comput. Chem.* **1989**, *10*, 982−1012.

(20) Gasteiger, J.; Marsili, M. Iterative Partial Equalization of Orbital Electronegativity - A Rapid Access to Atomic Charges. *Tetrahedron* **1980**, *36*, 3219−3288.

(21) Mohler, H.; Okada, T. Benzodiazepine Receptor: Demonstration in the Central Nervous System. *Science* **1977**, *198*, 849−851.

(22) Anzini, M.; Cappelli, A.; Vomero, S.; Cagnotto, A.; Skorupska, M. Synthesis and Benzodiazepine Receptor Affinity of 2,3-Dihydro-9-phenyl-1H-pyrrolo[3,4-b]quinolin-1-one and 3-Carbethoxy-4-phenylquinoline Derivatives. *Farmaco* **1992**, *47*, 191−202.

(23) (a) Basile, A. S.; Klein, D. C.; Skolnick, P. Characterization of Benzodiazepine Receptors in the Bovine Pineal Gland: Evidence for the Presence of an Atypical Binding Site. *Mol. Brain Res.* **1986**, *1*, 127−135. (b) Basile, A. S.; Ostrowsky, N.; Skolnick, P. Aldosterone Reversible Decrease in the Density of Renal Peripheral Benzodiazepine Receptors in the Rat After Adrenalectomy. *J. Pharmacol. Exp. Ther.* **1987**, *240*, 1006−1013.

JM960325J